Research Square

Preprints are preliminary reports that have not undergone peer review.
They should not be considered conclusive, used to inform clinical practice,
or referenced by the media as validated information.

IMU-Based Hip Adduction and Flexion Moment Estimation for Osteoarthritis and Healthy Individuals During Normal and Modified Gait

Chenquan Xu
Shanghai Jiao Tong University
Zhongtian Yu
Kyoto University
Yuanshuo Tan
Shanghai Jiao Tong University
Kezhe Zhu
Shanghai Jiao Tong University
Hong Wang
Shanghai Jiao Tong University
Qiqi Lu
Shanghai Sixth People's Hospital
Yueyuan Chen
Shanghai Jiao Tong University
Ziheng Xu
Shanghai Jiao Tong University
Guoxing Liu
Shanghai Jiao Tong University
Hai Hu
Shanghai Sixth People's Hospital
Peter B. Shull
pshull@sjtu.edu.cn

Chinese University of Hong Kong, Shenzhen
Hiroshige Tateuchi
Kyoto University

Research Article

Keywords: Hip osteoarthritis, rehabilitation, wearable sensors, inertial measurement units, gait biomechanics, hip joint moments, deep learning, few-shot personalization

Posted Date: September 10th, 2026

DOI: https://doi.org/10.21203/rs.3.rs-10762760/v1

License: This work is licensed under a Creative Commons Attribution 4.0 International License.
Read Full License

Additional Declarations: No competing interests reported.

IMU-Based Hip Adduction and Flexion Moment Estimation for Osteoarthritis and Healthy Individuals During Normal and Modified Gait

Chenquan Xu[1], Zhongtian Yu[3], Yuanshuo Tan[1], Kezhe Zhu[1], Hong Wang[1], Qiqi Lu[2], Yueyuan Chen[1], Ziheng Xu[1], Guoxing Liu[1], Hai Hu[2], Peter B. Shull[4,1*], Hiroshige Tateuchi[3]

[1]State Key Laboratory of Mechanical System and Vibration, School of Mechanical Engineering, Shanghai Jiao Tong University, Shanghai, 200240, China.

[2]Biomechanical Laboratory of Orthopedic Surgery Department, Shanghai Jiao Tong University School of Medicine Affiliated Sixth People's Hospital, Shanghai, China.

[3]Human Health Sciences, Graduate School of Medicine, Kyoto University, Kyoto, 606-8507, Japan.

[4]School of Artificial Intelligence, Chinese University of Hong Kong, Shenzhen, Shenzhen, 518172, China.

*Corresponding author(s). E-mail(s): pshull@sjtu.edu.cn;
Contributing authors: xiaoqin@sjtu.edu.cn;
yu.zhongtian.27s@st.kyoto-u.ac.jp; tanyuanshuo@sjtu.edu.cn;
kezhe_zhu@sjtu.edu.cn; hong_wang@sjtu.edu.cn; Dywane677@163.com;
yueyuanchen@sjtu.edu.cn; sjtuxzh0079@sjtu.edu.cn;
lgxing1900@sjtu.edu.cn; xmhuhai@hotmail.com;
tateuchi.hiroshige.8x@kyoto-u.ac.jp;

Abstract

Excessive cumulative hip joint loading and harmful compensatory gait patterns during daily activities often remain undetected outside the biomechanics laboratory, limiting timely adjustment of rehabilitation strategies and potentially accelerating disease progression in patients with hip osteoarthritis (HOA). Wearable inertial measurement units (IMUs) could enable continuous monitoring of hip joint loading, but accurate estimation must generalize across individuals,

pathological gait patterns, walking environments, and gait modifications. We recruited 84 participants (34 with osteoarthritis, 19 healthy older adults, and 31 healthy young adults) who performed normal and modified walking trials (fast and slow walking, toe-in and toe-out gait, wide and narrow step widths, increased lateral trunk sway, and dual-task walking) on an instrumented treadmill or overground force plates while wearing inertial measurement units (IMUs) and optical motion-capture markers. We developed a novel, personalized deep learning framework to estimate continuous hip adduction moment (HAM) and hip flexion moment (HFM) waveforms from input IMU signals at the trunk, pelvis, thigh, and shank. Personalization using only baseline walking data achieved RMSEs of 0.48 and 0.52 %BW·BH with waveform correlations of 0.96 and 0.94 for HAM and HFM, respectively. During independent overground evaluation, the personalized model achieved RMSEs of 0.92 and 0.77 %BW·BH with correlations of 0.91 and 0.93. Predicted peak moments and stance-phase moment impulses preserved gait-dependent differences across the evaluated gait modifications. By enabling individualized, low-burden hip-loading assessment across diverse gait patterns, this framework may help identify harmful compensatory strategies earlier, inform timely rehabilitation adjustments, broaden access to biomechanical monitoring outside specialized laboratories, and provide a technical basis for future wearable biofeedback and personalized rehabilitation assessment.

Keywords: Hip osteoarthritis, rehabilitation, wearable sensors, inertial measurement units, gait biomechanics, hip joint moments, deep learning, few-shot personalization

1 Introduction

Hip osteoarthritis (HOA) is a chronic, progressive, and highly disabling degenerative joint disease characterized by the gradual deterioration of articular cartilage, leading to severe pain and mobility impairment[1–3]. With a global pooled radiographic prevalence of approximately 8.55% that increases significantly with age[4], HOA stands as a leading cause of global disability among the aging population and poses a substantial socioeconomic burden[5, 6]. Consequently, there is an urgent clinical need for effective conservative treatments to mitigate symptoms and potentially slow functional and structural deterioration [7]. Abnormal dynamic joint loading during locomotion is recognized as a fundamental mechanical driver of HOA progression and symptom severity[8], while gait kinematic factors and excessive daily cumulative hip loading are also identified as critical prognostic factors predicting the subsequent radiographic progression[9].

Individuals with HOA often adopt compensatory gait strategies, including altered walking speed, reduced step length, modified pelvic motion, and increased ipsilateral trunk lean during the affected stance phase[2, 10, 11]. Such adaptations may reduce mechanical demand in one dimension while introducing altered loading patterns elsewhere in the musculoskeletal system. Additionally, abnormal hip joint loading may persist even after total hip replacement and may not be identifiable through routine clinical examination or static radiographic measures alone [12]. These challenges

highlight the need for individualized gait assessment to identify patient-specific movement strategies and guide targeted rehabilitation [13, 14]. Of particular interest are the hip adduction moment (HAM) and hip flexion moment (HFM). HAM has been used to assess frontal-plane cumulative loading and structural progression [9, 15], whereas HFM characterizes sagittal-plane muscular demand and has been associated with patient symptoms [8, 10]. Reliable estimation of stance-phase HAM and HFM waveforms may therefore support evaluation of gait modification strategies and rehabilitation-related changes in hip loading.

Conventionally, hip joint moments are estimated using optical motion capture (OMC) systems combined with force plates (FP) and inverse dynamics. Although these systems provide well-established laboratory measurements, their cost, setup requirements, limited capture volume, and dependence on instrumented environments restrict their use in routine clinical and ambulatory applications. Instrumented treadmill testing can capture consecutive strides but may be challenging for patients with pain, balance deficits, or limited mobility, and treadmill walking may differ from natural overground gait[16]. Conversely, overground force-plate assessments typically capture only a few valid foot contacts and may require repeated trials or conscious foot placement, potentially altering natural gait[17]. As a result, laboratory assessments provide only brief and highly controlled snapshots of gait that may not represent the variability in hip loading and compensatory strategies encountered during daily activities or rehabilitation, limiting opportunities for timely and individualized rehabilitation adjustment. Wearable inertial measurement units (IMUs) therefore offer a portable, low-cost, and low-burden means of extending hip-moment assessment from specialized laboratories to routine clinical and ambulatory settings.

Deep learning enables joint kinetics to be estimated directly from multidimensional IMU time series without requiring a complete analytical musculoskeletal modeling pipeline [18]. Recent studies have moved beyond isolated discrete outcomes toward complete joint-moment waveform estimation, preserving the magnitude, timing, and temporal evolution of joint demand [19–27]. Waveform reconstruction also enables clinically interpretable features, such as peak magnitude, peak timing, and stance-phase moment impulse, to be derived for gait assessment, phase-specific feedback, and assistive-control applications. Mundt et al. evaluated representative architectures, including MLPs, LSTMs, and CNNs, for three-dimensional lower-limb kinematic and kinetic estimation from measured and simulated IMU data during walking[20]. More recent studies broadened the task scope: Altai et al. evaluated XCM and related time-series models[24], Molinaro et al. employed a TCN[22], Hossain et al. developed a CNN-RNN ensemble[25], Wang et al. proposed a TCN-BiLSTM[23], Liang et al. demonstrated single-IMU estimation[27], and Tang et al. introduced a TCN-xLSTM architecture[26]. Collectively, these approaches have demonstrated promising joint-moment waveform estimation across level walking, speed variations, ramps, and stairs. However, they have been evaluated predominantly in healthy cohorts and conventional locomotor tasks, leaving their performance in unseen individuals with OA and during rehabilitation-related gait modifications insufficiently established.

For wearable deep learning systems to support HOA rehabilitation, they must remain accurate under cross-subject and cross-condition distribution shifts. Cross-subject variation arises from differences in anthropometry [28, 29], disease presentation [30], and patient-specific lower-limb coordination strategies [10], which may cause pathological gait patterns of a new patient to differ substantially from the training distribution. Cross-condition variation results from rehabilitation-related gait modifications, such as changes in walking speed, foot progression angle (FPA), step width, and trunk lean, to alter targeted hip-loading metrics [13, 14, 31, 32]. A clinically useful estimator should therefore generalize to new individuals while retaining accuracy across gait modifications.

Few-shot personalization offers a potential solution by adapting a population-level model using a small amount of calibration data from the target individual[33–37]. Related studies have demonstrated data-efficient user adaptation in wearable activity recognition [34, 35] and continuous biomechanical signal estimation, including IMU-based lower-limb kinematics and muscle-activation waveforms [36, 37]. Collecting calibration data for every rehabilitation-related gait modification would remain burdensome and clinically impractical. We therefore investigate a baseline-only personalization strategy, in which a population-level model is adapted using only a few habitual walking cycles and then applied to gait conditions excluded from subject-specific calibration. We hypothesize that baseline walking would provide sufficient information to calibrate relatively stable subject-specific characteristics, such as anthropometric scaling, sensor alignment, and habitual intersegmental coordination, while pretraining across diverse gait modifications would support generalization beyond the calibration condition.

Accordingly, we developed a few-shot personalization framework for IMU-based estimation of stance-phase HAM and HFM waveforms. We recruited 84 participants, including individuals with OA, healthy older adults, and healthy young adults, and collected synchronized IMU, OMC, and force data during normal walking and gait modifications, including fast and slow walking, toe-in and toe-out gait, wide and narrow step widths, increased lateral trunk sway, and dual-task walking. The proposed model was trained and internally evaluated using the treadmill cohort and externally evaluated using an independent overground cohort. For each unseen participant, the model was personalized using only baseline walking cycles and then evaluated on the remaining baseline cycles and gait-modification conditions excluded from subject-specific calibration. We hypothesized that baseline-only personalization would improve waveform accuracy relative to the subject-general model and improve estimation of peak moments and stance-phase moment impulses across normal and modified gait.

2 Methods

2.1 Subjects

Eighty-four individuals participated in this study, including 34 participants with OA, 19 healthy older adults, and 31 healthy young adults (Table 1). The treadmill cohort, used for population-model training and internal evaluation, comprised 63 participants (29 male and 34 female; age: 44.4 ± 14.9 years; height: 1.66 ± 0.08 m; mass: 65.9 ± 11.3

Table 1: Participant Characteristics for Treadmill and Overground Cohorts

Participant Group	Gender (M/F)	Age (years)	Height (m)	Weight (kg)	Baseline Speed (m/s)
Treadmill Walking					
Healthy Young Adults ($n = 19$)	11/8	23.8 ± 2.0	1.71 ± 0.07	64.6 ± 11.0	1.17 ± 0.09
Healthy Older Adults ($n = 19$)	9/10	55.2 ± 6.1	1.63 ± 0.07	63.3 ± 12.0	0.80 ± 0.12
Participants with OA ($n = 25$)	9/16	51.9 ± 7.6	1.65 ± 0.07	68.8 ± 10.9	0.70 ± 0.15
Overground Walking					
Healthy Young Adults ($n = 12$)	7/5	24.9 ± 2.4	1.69 ± 0.09	65.7 ± 10.0	–
Participants with OA ($n = 9$)	0/9	48.3 ± 13.8	1.57 ± 0.05	50.9 ± 6.6	–

Data are presented as mean ± standard deviation. –: Not available.

kg; BMI: 23.8 ± 3.2 kg/m^2), including 25 participants with lower-limb OA, 19 healthy older adults, and 19 healthy young adults. The independent overground cohort, used exclusively for external personalization and evaluation, comprised 21 participants (7 male and 14 female; age: 35.0 ± 14.9 years; height: 1.64 ± 0.09 m; mass: 59.3 ± 11.3 kg; BMI: 22.0 ± 2.9 kg/m^2), including nine participants with hip OA or developmental dysplasia of the hip (DDH) and 12 healthy young adults. No participant in the overground cohort was included in population-model training or internal evaluation.

Participants were recruited through the outpatient clinic of Shanghai Sixth People's Hospital and the outpatient clinic of Kyoto University Hospital. For participants with OA, the inclusion criteria were persistent joint pain on most days during the preceding month, radiographic evidence of OA, and the ability to walk independently without an assistive device. Participants enrolled in the treadmill experiment were additionally required to complete the treadmill walking protocol safely. Hip OA and DDH diagnoses in the overground cohort were confirmed through clinical and radiographic assessment. All participants provided written informed consent before data collection. The treadmill protocol was approved by the Ethics Committee of Shanghai Sixth People's Hospital, and the overground protocol was approved by the Ethics Committee of Kyoto University Graduate School and Faculty of Medicine.

2.2 Experimental Setup

2.2.1 Motion Capture and Force Plates

Three-dimensional marker trajectories were recorded at 100 Hz using either an eight-camera Qualisys system (Qualisys AB, Gothenburg, Sweden) or a ten-camera Vicon system (Oxford Metrics Group, Oxford, UK), depending on the experimental site. 65 retroreflective markers and rigid tracking clusters were placed on specific anatomical landmarks to define the segments: posterior surface of the calcaneus, head of the second metatarsal, head of the fifth metatarsal, tuberosity of the fifth metatarsal, fibula apex of lateral and tibia apex of medial malleoli, lateral and medial femoral epicondyles, greater trochanters, left and right anterior superior iliac spines, left and right posterior superior iliac spines, sternum jugular notch, left and right acromion, seventh cervical vertebra, sternum xiphisternal joint, and midway between the inferior angles of most caudal points of the two scapulae. Additionally, rigid marker clusters were placed on the bilateral thighs and shanks.

Ground reaction forces were recorded synchronously at 1000 Hz. For the treadmill cohort, forces were measured using a dual-belt instrumented treadmill (Bertec Corp., Worthington, OH, USA). For the overground cohort, forces were recorded using floor-embedded force plates (Kistler Group, Winterthur, Switzerland).

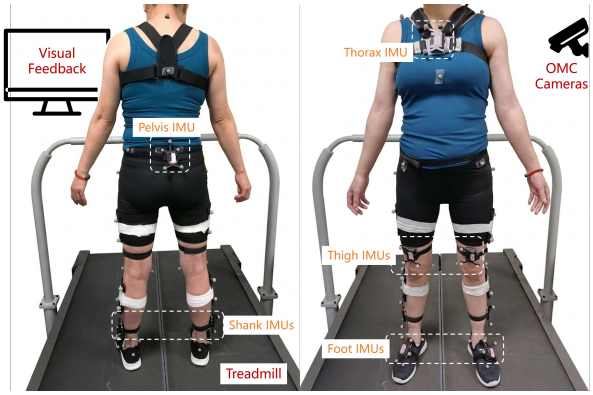


Fig. 1: Experimental setup. Participants walked on an instrumented treadmill while performing gait modifications with real-time visual feedback. Eight IMUs, an OMC system, and embedded force plates were used for data collection.

2.2.2 Inertial Measurement Units

Eight IMUs (SageMotion, Kalispell, MT, USA) recorded tri-axial acceleration and angular velocity at 100 Hz. The sensors were secured using elastic straps and positioned on the trunk (anterior chest), pelvis (lower back), and bilaterally on the anterior thighs (5 cm proximal to the patella), lateral shanks (5 cm proximal to the lateral malleolus), and the dorsum of the feet (Figure 1). Only the trunk, pelvis, and right thigh, shank, and foot IMUs were used for model development and evaluation. The sensor coordinate systems were standardized such that the positive y-axis directed upward, and the z-axis conformed to the right-hand rule.

2.3 Experimental Protocol

Two independent experiments were conducted using separate treadmill and over-ground cohorts.

2.3.1 Treadmill experiment

Participants completed a series of walking trials on an instrumented treadmill while wearing standardized attire and shoes. Prior to data collection, participants completed a two-minute warm-up to familiarize themselves with the treadmill and establish their preferred walking speed. The baseline trial consisted of one minute of walking at each participant's self-selected speed, and data from this trial were used to determine the baseline values of the targeted gait parameters.

Participants subsequently performed nine modified walking conditions: fast and slow walking (baseline ± 0.2 m/s), toe-in and toe-out gait (baseline FPA ± 10°), wide (baseline + 0.070 m) and narrow (baseline - 0.054 m) step widths, increased lateral trunk sway (baseline + 4° and + 8°), and a dual-task cognitive condition. During the dual-task condition, participants walked at their baseline speed while continuously counting backward by threes. Each trial lasted one minute, with adequate rest provided between trials as needed.

2.3.2 Overground experiment

A separate cohort performed overground walking trials along a level walkway under the baseline and modified gait conditions described above, except for the dual-task condition. Participants walked repeatedly in both directions, with the left and right limbs assessed in separate passes. A pass was considered valid when the designated foot fully contacted the force plate without simultaneous contact from the contralateral foot. For each trial, healthy participants completed 10 valid passes per limb, whereas participants with hip OA or DDH completed five valid passes per limb to reduce fatigue. Rest was provided between trials as required.

During the FPA, step width, and trunk sway conditions in both experiments, participants modified their gait using real-time visual feedback synchronized with the optical motion capture system and displayed on a front-facing monitor (Figure 1). Before each modified walking condition, participants practiced the required adjustment to ensure that they understood the task and could accurately interpret and respond to the feedback. During formal data collection, participants were instructed to modify only the targeted parameter while maintaining their baseline walking pattern for all other gait characteristics.

2.4 Data Preprocessing

2.4.1 Signal Synchronization and Gait Segmentation

Kinematic and kinetic data were processed in Visual3D (C-Motion, Germantown, MD, USA) to identify gait events and compute reference hip adduction and flexion moments. The IMU data were temporally aligned with the motion capture data by cross-correlating the corresponding right-shank angular velocity signals recorded during three preparatory leg swings before each trial. After synchronization, all data streams were resampled to 100 Hz and segmented into discrete stance-phase windows from heel strike to toe-off. Each target stance phase was retained together with 20 frames (0.20 s) before initial contact and 20 frames after toe-off to preserve information surrounding the stance transitions.

Windows containing missing samples or sustained abrupt signal discontinuities were excluded. All retained windows were subsequently zero-padded at the end of the sequence to a uniform maximum length of 176 frames. A binary mask was applied during model training and evaluation to prevent padded samples from contributing to the loss and performance metrics. Following preprocessing and quality control, 31,666 steps were retained in the treadmill dataset, corresponding to an average of approximately 54 steps per participant per trial, and 1,264 steps were retained in the overground

dataset. Only right-limb steps were included in the analysis. The corresponding right hip adduction and flexion moment waveforms were used as the prediction targets. Left-limb IMU signals and joint moments were not included.

2.4.2 Extraction of Gait Parameters

Gait parameters were extracted from the marker trajectories for each gait cycle. The foot progression angle was calculated from the horizontal projection of the vector connecting the calcaneus and second metatarsal markers and averaged over the predefined early-stance interval. Step width was calculated as the mediolateral distance between the bilateral calcaneus markers during the initial double-support phase. Trunk sway was defined as the frontal-plane angular range between the vertical axis and the pelvic-manubrium axis. Overground walking speed was calculated from the horizontal displacement of the pelvis divided by the corresponding elapsed time, whereas treadmill walking speed was obtained directly from the treadmill setting.

2.5 Proposed Model and Evaluation

2.5.1 Model Architecture

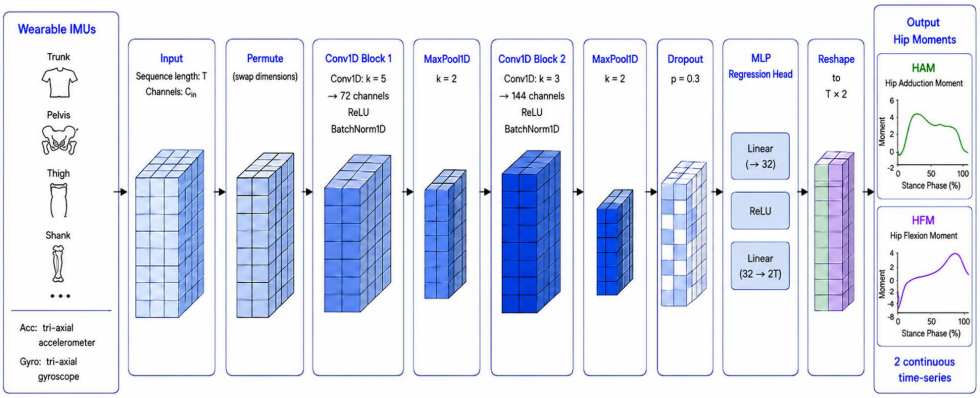


Fig. 2: Architecture of the proposed model for continuous HAM and HFM waveform estimation from wearable IMU signals through Conv1D feature extraction and an MLP regression head.

A one-dimensional convolutional neural network combined with a multilayer perceptron regression head (1DCNN-MLP) was developed to estimate stance-phase hip-moment waveforms from wearable IMU signals (Figure 2). A preliminary leave-one-location-out analysis was used to select the model inputs from the trunk, pelvis, right thigh, right shank, and right foot sensors. The trunk–pelvis–right thigh–right shank configuration achieved the lowest mean rRMSE across HAM and HFM and was therefore used for subsequent analyses. For each step window, tri-axial acceleration and angular velocity signals from four IMUs were concatenated along the channel

dimension to form a multichannel temporal input sequence. The model consisted of a temporal convolutional encoder followed by an MLP-based regression head. The encoder comprised two 1D convolutional layers: the first layer applied a kernel size of 5 to extract 72 feature channels, while the second layer used a kernel size of 3 to expand the representation to 144 channels. Each convolutional layer was followed by a rectified linear unit (ReLU) activation function, batch normalization to stabilize training, and max pooling for temporal downsampling. Dropout was subsequently applied to the encoded feature maps to prevent overfitting. The encoded temporal feature maps were flattened and passed to an MLP regression head containing one fully connected hidden layer with 32 units and ReLU activation. The final linear layer directly predicted two moment sequences, corresponding to HAM and HFM.

The proposed model was trained in a supervised manner using the Adam optimizer and mean squared error loss. The number of convolutional channels, fully connected units, learning rate, batch size, dropout probability, and training epochs were tuned jointly via a tree-structured Parzen estimator using leave-five-subject-out cross-validation within the treadmill cohort (Table 2). All steps from each participant were retained within the same fold, and the optimization objective was the average HAM and HFM rRMSE computed across all steps pooled from the held-out participants. Within each fold, a min–max scaler with a feature range of $[-1, 1]$ was fitted using only the training participants and then applied to the held-out participants. The model was implemented in Python 3.10 using PyTorch 2.3.0.

Table 2: Hyperparameter search space and selected values

Hyperparameter	Search Distribution	Selected Value
Epochs	$\mathcal{QU}(5, 15, 1)$	12
Learning Rate	$\mathcal{U}(1e-3, 1e-2)$	$3e-3$
Batch Size	$\mathcal{QU}(20, 80, 10)$	60
Fully Connected Units	$\mathcal{QN}(30, 10, 1)$	32
Dropout Probability	$\mathcal{QU}(0.1, 0.5, 0.1)$	0.3
CNN Channels	$\mathcal{QN}(64, 20, 8)$	72

$\mathcal{U}(a, b)$: uniform distribution between a and b.
$\mathcal{QU}(a, b, q)$: quantized uniform distribution with step size q.
$\mathcal{QN}(\mu, \sigma, q)$: quantized normal distribution with mean μ, standard deviation σ, and quantization step q.

2.5.2 Performance Evaluation

Subject-general performance was evaluated using a leave-five-subject-out cross-validation protocol on the treadmill dataset cohort. If the number of remaining subjects in the final fold was smaller than five, all remaining subjects were included in the final held-out fold. Within each fold, all available steps from the training subjects were concatenated and shuffled before mini-batch training. For each subject, all stance-phase samples across the evaluated trials were pooled to compute waveform-level

RMSE, rRMSE, and r. Subject-level metrics were then summarized across subjects as mean and standard error.

The effect of training-set size on generalization to unseen patients was evaluated using a patient-outer five-fold protocol to enable paired comparisons across training-participant proportions while preventing subject-level data leakage. Participants with OA were divided into five mutually exclusive folds, with approximately 20% held out for testing in each fold. For each fold, different proportions of the available training participants were randomly sampled to construct the reduced training sets, while the same held-out participants with OA were used for evaluation across all training-set sizes. Performance was summarized across the five folds using rRMSE and waveform correlation.

Gait-pattern-dependent analyses were performed for stance-phase waveforms, peak moments, and hip moment impulses. Steps were binned separately for each gait parameter. For FPA, step width, and trunk sway, steps from the corresponding modification trials were ranked by the measured step-level parameter and divided into three approximately equal-sized bins: toe-in, normal, and toe-out for FPA; narrow, normal, and wide for step width; and small, medium, and large for trunk sway. For treadmill walking, slow, normal, and fast groups were defined by the prescribed speed trials, with an equal number of steps randomly sampled from each condition for every participant. For overground walking, steps were ranked by measured step-level speed and divided into three approximately equal-sized bins.

For waveform analysis, each stance phase was resampled to 101 points. For peak analysis, peak HAM was defined as the first stance-phase adduction peak, whereas peak HFM was defined as the peak internal hip extension moment during stance, as both account for a large proportion of total hip joint contact force[38]. For impulse analysis, the cumulative hip moment impulse was computed as $\sum_t |M_t|\Delta t$ over the stance phase, with $\Delta t = 0.01$ s. The predicted and reference waveform, peak and impulse values were then compared across gait-pattern groups to evaluate whether the model preserved both instantaneous and cumulative biomechanical characteristics.

2.6 Baseline Models

The proposed model was compared with five baseline architectures commonly used for time-series biomechanical estimation: FCNN [19], LSTM[22], TCN [22], TCN-BiLSTM [23], and 2DCNN [21]. All baseline models used the same IMU inputs, output targets, preprocessing pipeline, data partitions, and optimization procedure as the proposed model. The FCNN contained two hidden layers with 100 and 20 units. The LSTM contained two recurrent layers with 50 hidden units. The TCN used five residual temporal convolutional levels with 50 channels per level. The TCN-BiLSTM combined dilated temporal convolutions with a bidirectional LSTM. The 2DCNN used two convolutional layers followed by a fully connected regression head. Model performance was quantified using RMSE, rRMSE, and Pearson correlation coefficient.

2.7 Few-Shot Personalization and Evaluation

Within the treadmill cross-validation analysis, each held-out participant was personalized from the population model trained on the corresponding source participants. After completion of the internal analysis, a final population model was trained from scratch using data from all 63 treadmill participants and used as the common initialization for personalization in the independent overground cohort.

For each unseen target participant, all network layers were fine-tuned using N labeled baseline steps for 200 epochs with the Adam optimizer and a learning rate of 3×10^{-4}. The calibration steps were removed from the test set, and the remaining baseline steps and all gait-modification steps were reserved exclusively for evaluation. The 0-shot condition denoted direct application of the population model without personalization, whereas the 1-, 3-, 5-, and 10-shot conditions used the corresponding numbers of baseline calibration steps.

3 Results

3.1 Subject-General Performance on the Treadmill Dataset Cohort

Table 3: Performance of the proposed model and baseline architectures on the treadmill cohort

Method	HAM			HFM		
	RMSE	rRMSE	r	RMSE	rRMSE	r
Subject-general models						
FCNN	1.02 (0.04)	11.3 (0.4)	0.85 (0.01)	1.05 (0.04)	10.2 (0.5)	0.86 (0.01)
2DCNN	0.81 (0.04)	9.1 (0.4)	0.92 (0.00)	0.94 (0.04)	9.2 (0.4)	0.90 (0.01)
LSTM	0.85 (0.04)	9.5 (0.4)	0.92 (0.00)	1.01 (0.04)	9.9 (0.5)	0.89 (0.01)
TCN	0.84 (0.04)	9.4 (0.5)	0.92 (0.00)	0.96 (0.04)	9.4 (0.5)	0.90 (0.01)
TCN-BiLSTM	0.91 (0.05)	10.2 (0.5)	0.89 (0.02)	1.06 (0.05)	10.2 (0.5)	0.86 (0.02)
Proposed Model	0.73 (0.04)†	8.2 (0.4)†	0.95 (0.00)†	0.86 (0.04)†	8.4 (0.5)†	0.92 (0.01)†
Personalized model						
Proposed Model + 10-shot finetune	0.48 (0.01)‡	5.4 (0.1)‡	0.96 (0.00)‡	0.52 (0.01)‡	5.0 (0.1)‡	0.94 (0.00)‡

Metrics are reported as mean and standard error across participants.
$^{\dagger}p < 0.01$ compared with all subject-general baseline models. $^{\ddagger}p < 0.01$ compared with the subject-general proposed model.

The proposed model achieved the lowest subject-general prediction errors among the evaluated models for both HAM and HFM (Table 3). For HAM, it obtained an RMSE of 0.73 %BW·BH and an rRMSE of 8.2%, outperforming the 2DCNN, which achieved 0.81 %BW·BH and 9.1%, respectively. For HFM, the proposed model achieved an RMSE of 0.86 %BW·BH and an rRMSE of 8.4%, compared with 0.94 %BW·BH and 9.2% for the 2DCNN. It also achieved the highest waveform correlations for HAM ($r = 0.95$) and HFM ($r = 0.92$). Relative to the TCN baseline, the proposed model reduced rRMSE from 9.4% to 8.2% for HAM and from 9.4% to 8.4% for HFM.

The model also preserved condition-dependent waveform patterns across gait modifications. Across step-width, trunk-sway, and walking-speed conditions, predicted

HAM waveforms generally followed the corresponding inverse-dynamics reference patterns (Figure 3).

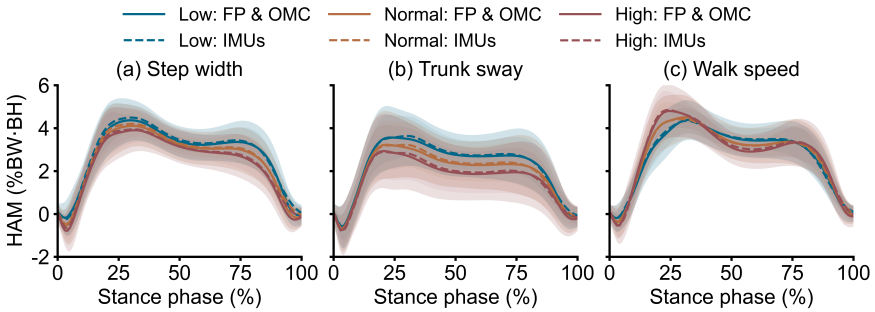


Fig. 3: HAM waveform estimation across gait modification conditions. Shaded regions represent inter-subject variability. Predicted waveforms followed the condition-dependent trends observed in the reference measurements.

3.2 Personalized Estimation Across Treadmill and Overground Cohorts

The effect of personalization was reflected in overall waveform accuracy and calibration-set size. In the treadmill cohort, one-shot personalization produced only marginal changes relative to the 0-shot model, whereas 3-shot personalization reduced rRMSE from 8.1% to 5.5% for HAM and from 8.5% to 5.2% for HFM. For both moments, the rRMSE reductions and waveform correlation increases from 0-shot to 3-shot and from 3-shot to 10-shot were statistically significant. Ten-shot personalization further reduced rRMSE to 5.4% for HAM and 5.0% for HFM, with smaller additional improvements in waveform correlation (Table 3, Figure 4).

Pairwise group comparisons showed that residual population-dependent differences remained after 10-shot personalization. For HAM, patients had significantly higher rRMSE than young and older subjects. For HFM, patients had significantly higher rRMSE and lower correlation coefficients than both young and older subjects, with an additional reduction in correlation observed in older compared with young subjects.

Consistent improvements were observed across all evaluated gait conditions for the stance-phase waveform, peak moment, and moment impulse (Appendix A Table A1). Across conditions, HAM waveform RMSE decreased from 0.67–0.82 to 0.41–0.65 %BW·BH, whereas HFM waveform RMSE decreased from 0.77–0.92 to 0.49–0.70 %BW·BH. Peak moment errors were also reduced; for example, during fast walking, HAM peak RMSE decreased from 1.09 to 0.81 %BW·BH and HFM peak RMSE decreased from 1.00 to 0.66 %BW·BH. The largest waveform and peak improvements were observed during fast walking, whereas the large-trunk-sway condition generally retained the highest post-personalization errors. Moment impulse RMSE also decreased for both moments under every gait condition.

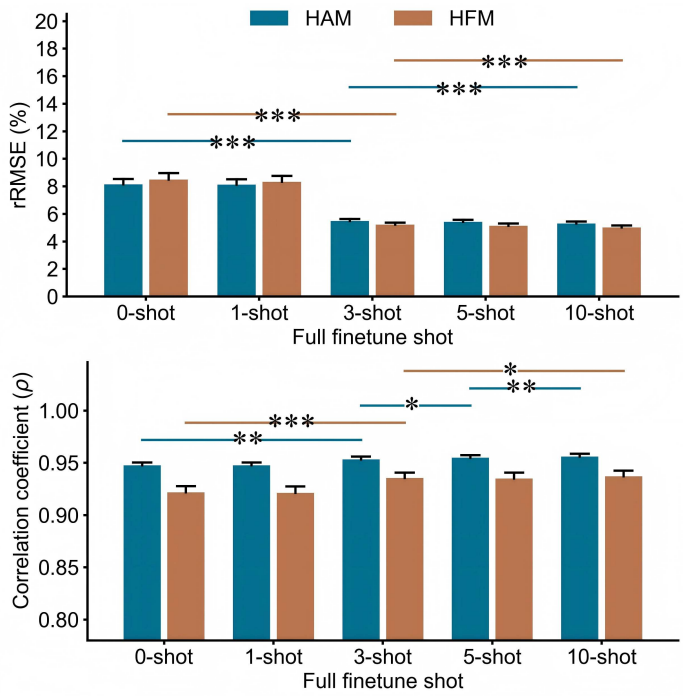


Fig. 4: Few-shot personalization evaluation. Bars represent the mean and one standard error across test subjects. Significance lines denote paired comparisons between shot conditions for which increasing the number of calibration steps improved performance, with $^{*}p < 0.05$, $^{**}p < 0.01$, and $^{***}p < 0.001$.

The personalized framework also generalized to the independent overground cohort. Compared with the non-finetuned model, 10-shot personalization reduced HAM RMSE and rRMSE from 1.56 ± 0.16 %BW·BH and 14.4 ± 1.2% to 0.92 ± 0.09 %BW·BH and 8.5 ± 0.5%, respectively. For HFM, RMSE and rRMSE decreased from 0.94 ± 0.07 %BW·BH and 7.5 ± 0.5% to 0.77 ± 0.06 %BW·BH and 6.2 ± 0.4%. Correlation coefficients remained high, around 0.91 for HAM and 0.93 for HFM.

Peak moment analysis further showed that the personalized model captured the expected modulation of hip moments across overground gait conditions (Figure 5). Predicted peak HAM and HFM values generally followed the inverse-dynamics reference trends across step-width, trunk-sway, and walking-speed conditions, indicating that the personalized IMU model preserved condition-dependent biomechanical variations. Neither the predicted nor reference peak moments differed significantly across the FPA bins.

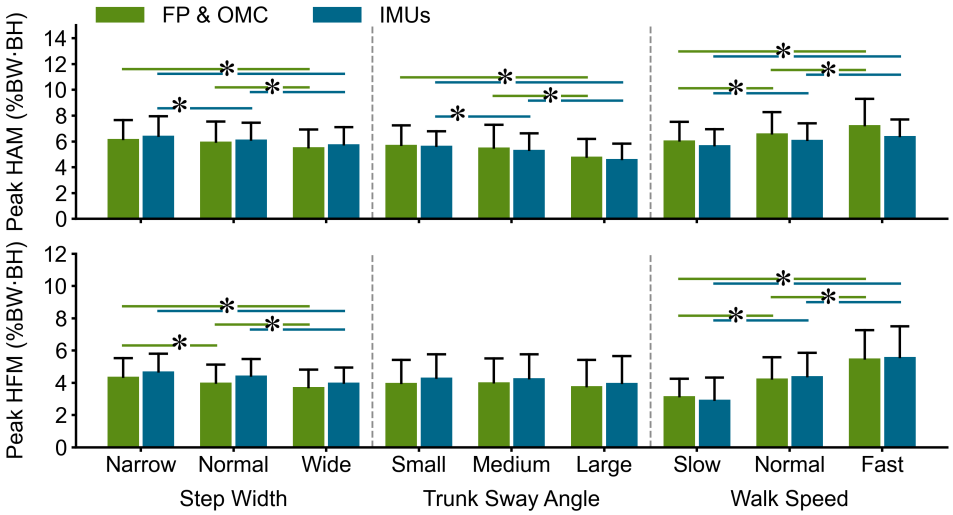


Fig. 5: Peak hip moment estimation across overground gait conditions after 10-shot personalization. Bars represent the mean and one standard deviation of the reference FP & OMC measurements and IMU-based predictions. Significance lines indicate statistical differences between gait conditions.

4 Discussion

4.1 Few-Shot Personalization and Biomechanical Relevance

Results indicate that a small number of labeled baseline calibration steps can provide useful subject-specific information for IMU-based hip-moment estimation. Baseline walking may capture stable features such as anthropometry, sensor orientation, intersegmental coordination, and subject-specific moment scaling between IMU signals and joint moments. Because these features are not limited to a single gait modification, baseline-only fine-tuning improved estimation across conditions that were excluded from calibration.

Personalization improved RMSE more than waveform correlation. This is expected because the subject-general model already achieved high correlations, leaving limited room to improve waveform shape agreement. RMSE is more sensitive to subject-specific amplitude bias, offsets, and scaling differences. Few-shot fine-tuning, therefore, appeared to correct subject-specific scaling and amplitude errors while preserving the temporal waveform structure learned by the population model.

The personalized estimates also retained biomechanically relevant information. Linear mixed-effects analyses identified positive associations between hip adduction angle (HAA) and both the reference and predicted HAM impulses (Figure 6). This relationship is biomechanically relevant because HAA reflects frontal-plane hip motion, whereas HAM impulse represents cumulative frontal-plane hip loading during stance.

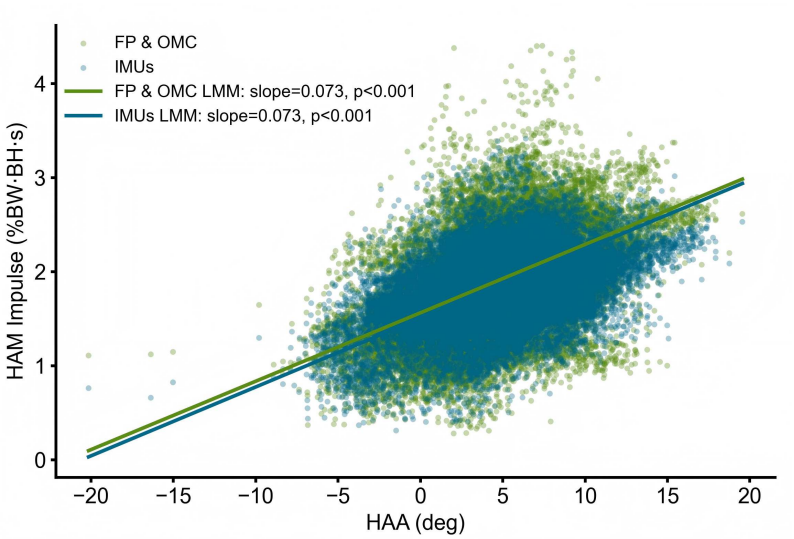


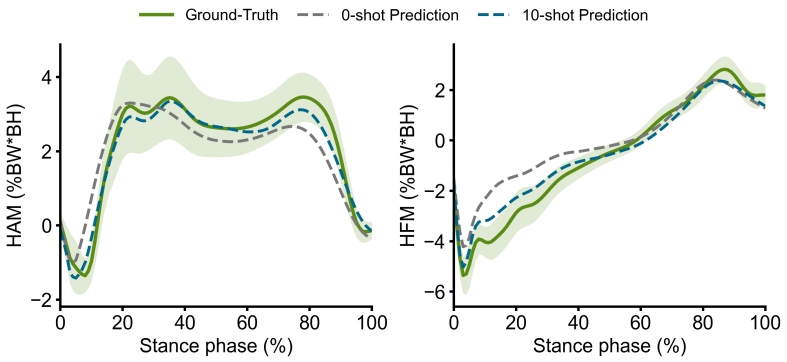
Fig. 6: Association between hip adduction angle and absolute HAM impulse. Linear mixed-effects models identified positive associations for both the reference FP & OMC measurements and IMU-based predictions.

The consistency between reference and predicted associations suggests that the personalized estimates retained meaningful hip-loading information, rather than only reducing waveform error. Illustrative participant-level examples further showed how 10-shot fine-tuning corrected subject-specific discrepancies in waveform and peak moment agreement (Figure 7). These examples complement the group-level results by showing how limited baseline calibration can adapt the population model to individual movement and sensor characteristics.

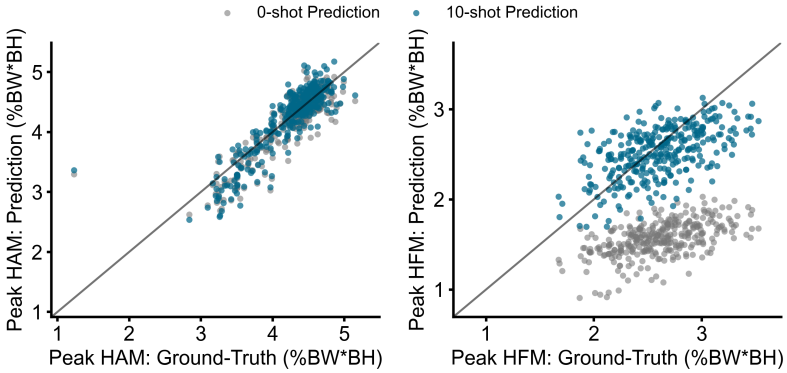
4.2 Sensor Configuration, Training Data, and Deployment Considerations

The incremental sensor configurations were defined based on the preceding leave-one-location-out analysis. The foot IMU provided the smallest additional benefit for hip-moment estimation, whereas the pelvis, thigh, trunk, and shank sensors contributed more consistently to model performance. The subsequent sensor-number comparison therefore used the following configurations: pelvis for 1IMU; pelvis and thigh for 2IMU; thigh, pelvis, and trunk for 3IMU; shank, thigh, pelvis, and trunk for 4IMU; and foot, shank, thigh, pelvis, and trunk for 5IMU.

The treadmill-based IMU-number comparison used leave-five-subject-out cross-validation without subject-specific fine-tuning and therefore reflects subject-general performance in unseen participants (Figure 8). Waveform correlations generally increased as additional sensor locations were included, with significant improvements from 1IMU to 2IMU and from 2IMU to 4IMU. These findings indicate



(a) Subject P019



(b) Subject P024

Fig. 7: Illustrative examples of few-shot personalization in the treadmill cohort. Zero-shot predictions were compared with 10-shot personalized predictions for two held-out participants. The examples illustrate changes in waveform and peak moment agreement after subject-specific fine-tuning.

that multi-segment motion signals provided complementary information for hip-moment estimation. The pelvis and thigh IMUs primarily captured hip-proximal motion, whereas the trunk and shank provided complementary information related to upper-body compensation, lower-limb progression, and stance timing. Consequently, performance improved substantially from 1IMU to 4IMU, while the additional foot IMU contributed only limited independent information.

The four-IMU configuration therefore provided a favorable balance between prediction accuracy and wearable burden. Although additional IMUs reduced prediction errors, the relatively high waveform correlations obtained with reduced configurations suggest that fewer sensors may remain useful for applications in which users adjust their gait according to relative changes in waveform shape rather than absolute moment magnitude.

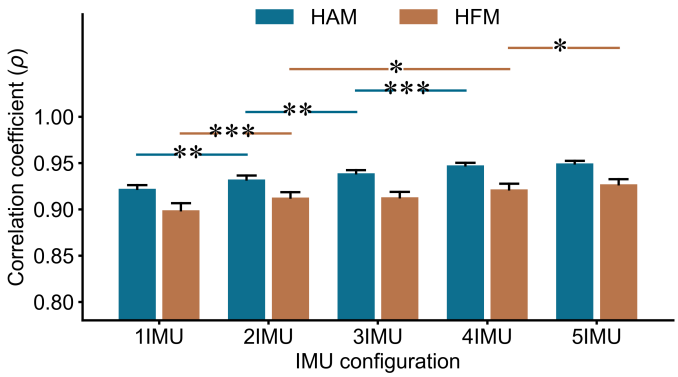
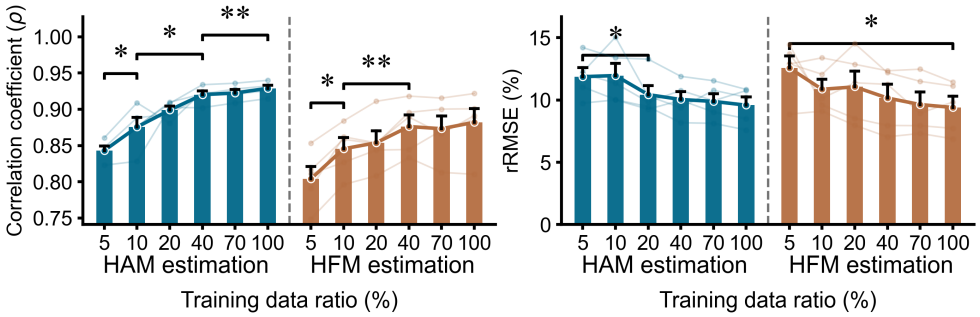


Fig. 8: Different IMU configuration for hip moment estimation. Bars represent the mean and one standard error across test subjects. Significance lines denote paired comparisons between IMU configurations for which increasing the number of IMUs improved performance, with $^{*}p < 0.05$, $^{**}p < 0.01$, and $^{***}p < 0.001$.

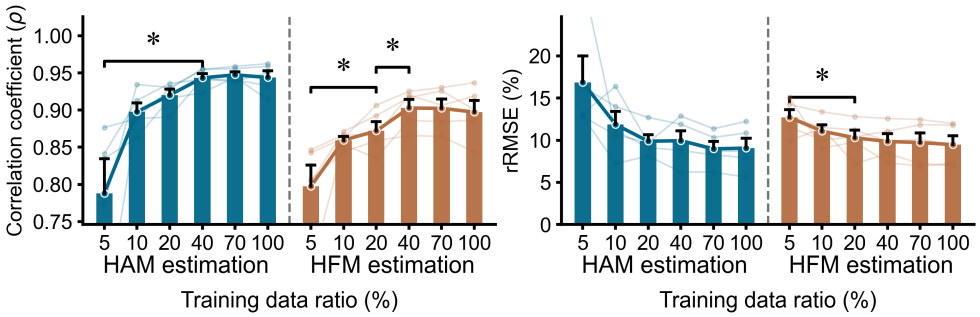
Increasing the proportion of training participants improved subject-general performance under both the one- and four-IMU configurations (Figure 9). This effect was more pronounced with a single pelvis IMU, suggesting that larger and more diverse training cohorts are particularly important when hip moments must be inferred from limited kinematic input. In contrast, the four-IMU configuration reached comparatively stable performance with a more moderate training-set size, likely because the trunk, pelvis, thigh, and shank signals provided complementary biomechanical information.

These results indicate that additional participants can partially compensate for limited sensor coverage, but training data and sensor information are not interchangeable. Larger datasets primarily improve robustness to inter-participant variability, whereas multi-segment sensing provides information that cannot be fully recovered from a single sensor. The diminishing gains at higher training proportions further indicate that dataset size alone does not determine performance once sufficient movement variability has been represented.

Training-population composition was also evaluated using the same patient-outer five-fold protocol. In each fold, five participants with OA were held out for testing, while separate models were trained using 19 healthy young adults, 19 healthy older adults, or 19 participants with OA. No consistent significant differences were observed among the training populations, possibly because within-group heterogeneity and the relatively small test set may have limited the ability to detect population-composition effects. The broad range of gait modifications represented in each training group may also have reduced differences between populations by exposing the model to diverse movement patterns. These findings suggest that diverse healthy-participant data may support population-model training when patient recruitment is limited.



(a) single-IMU configuration



(b) 4-IMU configuration

Fig. 9: Effect of training data size under single-IMU configuration and 4-IMU configuration. The training proportions corresponded to 3, 6, 12, 23, 41, and 58 participants, while five participants with OA were held out for testing in each fold. Bars represent the mean and one standard error across folds, and thin lines indicate fold-wise performance trends. Significance lines denote paired comparisons between training data proportions, with $*p < 0.05$, $**p < 0.01$, and $***p < 0.001$.

4.3 Advantages and Limitations

The present findings highlight the potential value of few-shot personalization for IMU-based hip-moment estimation. Few-shot personalization substantially reduced waveform, peak moment, and impulse errors using only baseline walking steps, while generalizing to gait modifications excluded from calibration.

The effect of personalization was not limited to waveform-level error reduction. The personalized model also improved the estimation of peak moments and moment impulses, maintained high waveform correlations in the independent overground cohort, reproduced condition-dependent changes in peak moments, and preserved the association between HAA and HAM impulse. These findings suggest that the estimated waveforms retained biomechanically meaningful information rather than only

reducing numerical prediction error. This is relevant for potential applications in gait retraining and rehabilitation monitoring, where peak loading, cumulative loading, and condition-dependent changes are more directly interpretable than waveform error alone.

The treadmill cohort included healthy young adults, healthy older adults, and participants with OA affecting different lower-limb joints, exposing the model to a broad range of compensatory gait strategies. This heterogeneous cohort was intentionally included because lower-limb joint mechanics are highly interdependent; knee OA alters hip and ankle kinetics and inter-joint coordination, whereas altered hip, pelvis, and trunk mechanics can also influence knee loading[39–41], and hip and knee OA frequently coexist [42]. The independent overground cohort further evaluated transferability across measurement systems, protocols, and participant characteristics. Together with the IMU-number and training-size analyses, these results provide practical guidance for designing wearable hip-moment estimation systems.

Several limitations should be considered. Reference hip moments were obtained from optical motion capture, force measurements, and inverse dynamics rather than direct measurement, and the treadmill and overground cohorts used different measurement systems and protocols. The experiments were conducted under controlled treadmill and force-plate-based overground conditions, which may not fully represent unconstrained daily walking [43]. Future work should evaluate bilateral and real-time implementation in larger clinical cohorts and investigate label-efficient or portable calibration strategies for daily-life use. In addition, the personalization procedure relied on laboratory-based baseline calibration. Future work should investigate self-supervised or unsupervised adaptation strategies that reduce or eliminate the need for labeled calibration data, and determine how cohort diversity, gait-condition coverage, and sensor placement can compensate for reduced sensor input while maintaining robustness across participants and walking conditions.

5 Conclusion

This study demonstrated that continuous hip adduction and flexion moment waveforms can be estimated from wearable IMUs using a few-shot personalized deep learning framework. The model was developed and evaluated using data from participants with osteoarthritis, healthy older adults, and healthy young adults during normal walking and modified gait, including fast and slow walking, toe-in and toe-out gait, wide and narrow step widths, increased lateral trunk sway, and dual-task walking. The subject-general model outperformed the evaluated baseline architectures, while personalization using only baseline gait cycles substantially improved waveform, peak moment, and moment impulse estimation across multiple gait patterns. The personalized model also maintained good performance in an independent overground cohort containing healthy participants and individuals with hip osteoarthritis or developmental dysplasia of the hip.

The proposed framework could facilitate individualized assessment of hip loading during gait retraining, rehabilitation monitoring, and out-of-laboratory biomechanical

evaluation. Future work should reduce the dependence on laboratory-based calibration and validate the system during real-time and unconstrained daily-life walking.

Declarations

Funding. This work was supported by the National Natural Science Foundation of China under Grant W2441018.

Competing interests. The authors declare that they have no competing interests.

Ethics approval and consent to participate. Treadmill data collection involving human participants was approved by the Institutional Review Board of Shanghai Sixth People's Hospital Ethics Committee under Application No. 2021-KY-71[K]. Overground data collection was approved by the Ethics Committee of Kyoto University Graduate School and Faculty of Medicine under approval no. R4597. All participants provided informed consent before participation.

Consent for publication. Not applicable.

Author contributions. C.X. and P.B.S. conceived and designed the study. Z.Y., K.Z., H.W., Q.L., Y.C., Z.X., G.L., H.H., and H.T. contributed to data collection and experimental implementation. Y.T. contributed to part of the data processing. C.X. performed data collection, data processing, model development, statistical analysis, interpretation of results, and manuscript drafting. P.B.S. supervised the study, acquired financial support, and revised the manuscript. All authors reviewed and approved the final manuscript.

Appendix A Trial-wise Personalization Performance

References

[1] Hall, M., Esch, M., Hinman, R.S., Peat, G., Zwart, A., Quicke, J.G., Runhaar, J., Knoop, J., Leeden, M., Rooij, M., Meulenbelt, I., Vliet Vlieland, T., Lems, W.F., Holden, M.A., Foster, N.E., Bennell, K.L.: How does hip osteoarthritis differ from knee osteoarthritis? Osteoarthritis Cartilage **30**(1), 32–41 (2022) https://doi.org/10.1016/j.joca.2021.09.010

[2] Steingrebe, H., Spancken, S., Sell, S., Stein, T.: Effects of hip osteoarthritis on lower body joint kinematics during locomotion tasks: a systematic review and meta-analysis. Frontiers in Sports and Active Living **5** (2023) https://doi.org/10.3389/fspor.2023.1197883

[3] Hunter, D.J., March, L., Chew, M.: Osteoarthritis in 2020 and beyond: a lancet commission. The Lancet **396**(10264), 1711–1712 (2020)

[4] Fan, Z., Yan, L., Liu, H., Li, X., Fan, K., Liu, Q., Li, J.J., Wang, B.: The prevalence of hip osteoarthritis: a systematic review and meta-analysis. Arthritis research & therapy **25**(1), 51 (2023)

Table A1: Trial-wise waveform, peak moment, and moment impulse RMSE before and after 10-shot personalization

Moment	Trial	Without personalization			10-shot personalization		
		Waveform	Peak	Impulse	Waveform	Peak	Impulse
HAM	Baseline	0.73 (0.04)	1.02 (0.09)	0.31 (0.03)	0.54 (0.02)	0.87 (0.10)	0.20 (0.01)
	Walk speed large	0.79 (0.05)	1.09 (0.09)	0.30 (0.03)	0.48 (0.02)	0.81 (0.11)	0.13 (0.01)
	Walk speed small	0.70 (0.04)	0.93 (0.07)	0.37 (0.04)	0.50 (0.03)	0.66 (0.06)	0.22 (0.03)
	FPA large	0.75 (0.04)	1.15 (0.09)	0.31 (0.02)	0.48 (0.02)	0.97 (0.11)	0.15 (0.01)
	FPA small	0.72 (0.04)	1.05 (0.09)	0.32 (0.03)	0.45 (0.02)	0.83 (0.10)	0.15 (0.01)
	Step width large	0.70 (0.04)	0.99 (0.07)	0.29 (0.02)	0.44 (0.02)	0.72 (0.08)	0.13 (0.01)
	Step width small	0.70 (0.04)	0.97 (0.08)	0.30 (0.03)	0.44 (0.01)	0.71 (0.08)	0.14 (0.01)
	Trunk sway large	0.82 (0.05)	1.02 (0.08)	0.36 (0.03)	0.65 (0.03)	0.86 (0.07)	0.25 (0.02)
	Trunk sway small	0.76 (0.05)	0.98 (0.08)	0.33 (0.03)	0.53 (0.02)	0.78 (0.10)	0.20 (0.01)
	Dual task	0.67 (0.04)	0.89 (0.09)	0.29 (0.03)	0.41 (0.01)	0.63 (0.11)	0.14 (0.01)
HFM	Baseline	0.82 (0.05)	0.80 (0.07)	0.27 (0.02)	0.65 (0.03)	0.65 (0.05)	0.21 (0.02)
	Walk speed large	0.92 (0.05)	1.00 (0.08)	0.27 (0.02)	0.57 (0.02)	0.66 (0.04)	0.13 (0.01)
	Walk speed small	0.77 (0.04)	0.61 (0.05)	0.26 (0.02)	0.53 (0.02)	0.44 (0.02)	0.16 (0.01)
	FPA large	0.82 (0.04)	0.75 (0.07)	0.24 (0.02)	0.52 (0.02)	0.49 (0.03)	0.13 (0.01)
	FPA small	0.84 (0.05)	0.78 (0.07)	0.27 (0.02)	0.50 (0.02)	0.52 (0.03)	0.13 (0.01)
	Step width large	0.80 (0.05)	0.72 (0.06)	0.24 (0.02)	0.49 (0.01)	0.44 (0.03)	0.11 (0.01)
	Step width small	0.81 (0.05)	0.79 (0.07)	0.26 (0.02)	0.49 (0.02)	0.53 (0.04)	0.13 (0.01)
	Trunk sway large	0.90 (0.04)	0.83 (0.07)	0.29 (0.03)	0.70 (0.03)	0.68 (0.05)	0.22 (0.02)
	Trunk sway small	0.84 (0.05)	0.78 (0.07)	0.27 (0.02)	0.58 (0.02)	0.59 (0.04)	0.18 (0.01)
	Dual task	0.83 (0.05)	0.75 (0.08)	0.26 (0.02)	0.49 (0.02)	0.45 (0.03)	0.13 (0.01)

Waveform and peak RMSE are reported in %BW·BH, whereas impulse RMSE is reported in %BW·BH·s. Metrics are reported as mean and standard error across participants.

[5] Cross, M., Smith, E., Hoy, D., Nolte, S., Ackerman, I., Fransen, M., Bridgett, L., Williams, S., Guillemin, F., Hill, C.L., *et al.*: The global burden of hip and knee osteoarthritis: estimates from the global burden of disease 2010 study. Annals of the rheumatic diseases **73**(7), 1323–1330 (2014)

[6] Moseng, T., Vlieland, T.P.V., Battista, S., Beckwée, D., Boyadzhieva, V., Conaghan, P.G., Costa, D., Doherty, M., Finney, A.G., Georgiev, T., *et al.*: Eular recommendations for the non-pharmacological core management of hip and knee osteoarthritis: 2023 update. Annals of the rheumatic diseases **83**(6), 730–740 (2024)

[7] Ackerman, I.N., Bohensky, M.A., Steiger, R., Brand, C.A., Eskelinen, A., Fenstad, A.M., Furnes, O., Graves, S.E., Haapakoski, J., Mäkelä, K., *et al.*: Lifetime risk of primary total hip replacement surgery for osteoarthritis from 2003 to 2013: a multinational analysis using national registry data. Arthritis care & research **69**(11), 1659–1667 (2017)

[8] Liao, T.-C., Samaan, M.A., Popovic, T., Neumann, J., Zhang, A.L., Link, T.M., Majumdar, S., Souza, R.B.: Abnormal joint loading during gait in persons with hip osteoarthritis is associated with symptoms and cartilage lesions. Journal of Orthopaedic & Sports Physical Therapy **49**(12), 917–924 (2019) https://doi.org/10.2519/jospt.2019.8945

[9] Tateuchi, H., Koyama, Y., Akiyama, H., Goto, K., So, K., Kuroda, Y., Ichihashi,

N.: Daily cumulative hip moment is associated with radiographic progression of secondary hip osteoarthritis. Osteoarthritis and Cartilage **25**(8), 1291–1298 (2017) https://doi.org/10.1016/j.joca.2017.02.796

[10] Watelain, E., Dujardin, F., Babier, F., Dubois, D., Allard, P.: Pelvic and lower limb compensatory actions of subjects in an early stage of hip osteoarthritis. Arch Phys Med Rehabil **82**(12), 1705–11 (2001) https://doi.org/10.1053/apmr.2001.26812

[11] Reininga, I.H., Stevens, M., Wagenmakers, R., Bulstra, S.K., Groothoff, J.W., Zijlstra, W.: Subjects with hip osteoarthritis show distinctive patterns of trunk movements during gait-a body-fixed-sensor based analysis. Journal of neuroengineering and rehabilitation **9**(1), 3 (2012)

[12] Stief, F., Schmidt, A., Drongelen, S., Lenarz, K., Froemel, D., Tarhan, T., Lutz, F., Meurer, A.: Abnormal loading of the hip and knee joints in unilateral hip osteoarthritis persists two years after total hip replacement. Journal of Orthopaedic Research® **36**(8), 2167–2177 (2018)

[13] Tateuchi, H., Akiyama, H., Goto, K., So, K., Kuroda, Y., Ichihashi, N.: Gait kinematics of the hip, pelvis, and trunk associated with external hip adduction moment in patients with secondary hip osteoarthritis: toward determination of the key point in gait modification. BMC Musculoskeletal Disorders **21**(1) (2020) https://doi.org/10.1186/s12891-019-3022-1

[14] Rynne, R., Le Tong, G., Cheung, R.T.H., Constantinou, M.: Effectiveness of gait retraining interventions in individuals with hip or knee osteoarthritis: A systematic review and meta-analysis. Gait Posture **95**, 164–175 (2022) https://doi.org/10.1016/j.gaitpost.2022.04.013

[15] Diamond, L.E., Allison, K., Dobson, F., Hall, M.: Hip joint moments during walking in people with hip osteoarthritis: a systematic review and meta-analysis. Osteoarthritis and Cartilage **26**(11), 1415–1424 (2018) https://doi.org/10.1016/j.joca.2018.03.011

[16] Parvataneni, K., Ploeg, L., Olney, S.J., Brouwer, B.: Kinematic, kinetic and metabolic parameters of treadmill versus overground walking in healthy older adults. Clinical Biomechanics **24**(1), 95–100 (2009) https://doi.org/10.1016/j.clinbiomech.2008.07.002

[17] Sanderson, D.J., Franks, I.M., Elliott, D.: The effects of targeting on the ground reaction forces during level walking. Human movement science **12**(3), 327–337 (1993)

[18] Halilaj, E., Rajagopal, A., Fiterau, M., Hicks, J.L., Hastie, T.J., Delp, S.L.: Machine learning in human movement biomechanics: Best practices, common pitfalls, and new opportunities. Journal of biomechanics **81**, 1–11 (2018)

[19] Mundt, M., Koeppe, A., David, S., Witter, T., Bamer, F., Potthast, W., Markert, B.: Estimation of gait mechanics based on simulated and measured imu data using an artificial neural network. Frontiers in Bioengineering and Biotechnology **8** (2020) https://doi.org/10.3389/fbioe.2020.00041

[20] Mundt, M., Johnson, W.R., Potthast, W., Markert, B., Mian, A., Alderson, J.: A comparison of three neural network approaches for estimating joint angles and moments from inertial measurement units. Sensors **21**(13), 4535 (2021) https://doi.org/10.3390/s21134535

[21] Dorschky, E., Nitschke, M., Martindale, C.F., Van Den Bogert, A.J., Koelewijn, A.D., Eskofier, B.M.: Cnn-based estimation of sagittal plane walking and running biomechanics from measured and simulated inertial sensor data. Frontiers in Bioengineering and Biotechnology **8** (2020) https://doi.org/10.3389/fbioe.2020.00604

[22] Molinaro, D.D., Kang, I., Camargo, J., Gombolay, M.C., Young, A.J.: Subject-independent, biological hip moment estimation during multimodal overground ambulation using deep learning. IEEE Transactions on Medical Robotics and Bionics **4**(1), 219–229 (2022) https://doi.org/10.1109/tmrb.2022.3144025

[23] Wang, F., Liang, W., Afzal, H.M.R., Fan, A., Li, W., Dai, X., Liu, S., Hu, Y., Li, Z., Yang, P.: Estimation of lower limb joint angles and joint moments during different locomotive activities using the inertial measurement units and a hybrid deep learning model. Sensors **23**(22), 9039 (2023) https://doi.org/10.3390/s23229039

[24] Altai, Z., Boukhennoufa, I., Zhai, X., Phillips, A., Moran, J., Liew, B.X.W.: Performance of multiple neural networks in predicting lower limb joint moments using wearable sensors. Frontiers in Bioengineering and Biotechnology **11** (2023) https://doi.org/10.3389/fbioe.2023.1215770

[25] Hossain, M.S.B., Guo, Z., Choi, H.: Estimation of lower extremity joint moments and 3d ground reaction forces using imu sensors in multiple walking conditions: A deep learning approach. IEEE Journal of Biomedical and Health Informatics **27**(6), 2829–2840 (2023) https://doi.org/10.1109/jbhi.2023.3262164

[26] Tang, Z., Wang, Y., Mao, S., Wei, D.: Tcn-xlstm: A hybrid temporal model integrating tcn and xlstm for lower limb joint moment estimation from imu signals. IEEE Robotics and Automation Letters **11**(1), 153–160 (2026) https://doi.org/10.1109/lra.2025.3632757

[27] Liang, W., Wang, F., Fan, A., Zhao, W., Yao, W., Yang, P.: Deep-learning model for the prediction of lower-limb joint moments using single inertial measurement unit during different locomotive activities. Biomedical Signal Processing and Control **86**, 105372 (2023) https://doi.org/10.1016/j.bspc.2023.105372

[28] Camomilla, V., Cereatti, A., Cutti, A.G., Fantozzi, S., Stagni, R., Vannozzi, G.:

Methodological factors affecting joint moments estimation in clinical gait analysis: a systematic review. BioMedical Engineering OnLine **16**(1) (2017) https://doi.org/10.1186/s12938-017-0396-x

[29] Hafer, J.F., Vitali, R., Gurchiek, R., Curtze, C., Shull, P., Cain, S.M.: Challenges and advances in the use of wearable sensors for lower extremity biomechanics. Journal of biomechanics **157**, 111714 (2023)

[30] Meyer, C.A.G., Corten, K., Fieuws, S., Deschamps, K., Monari, D., Wesseling, M., Simon, J.-P., Desloovere, K.: Biomechanical gait features associated with hip osteoarthritis: Towards a better definition of clinical hallmarks. Journal of Orthopaedic Research **33**(10), 1498–1507 (2015) https://doi.org/10.1002/jor.22924 https://onlinelibrary.wiley.com/doi/pdf/10.1002/jor.22924

[31] Tan, T., Wang, D., Shull, P.B., Halilaj, E.: Imu and smartphone camera fusion for knee adduction and knee flexion moment estimation during walking. IEEE Transactions on Industrial Informatics **19**(2), 1445–1455 (2023) https://doi.org/10.1109/TII.2022.3189648

[32] Inai, T., Takabayashi, T., Edama, M., Kubo, M.: Evaluation of factors that affect hip moment impulse during gait: A systematic review. Gait & Posture **61**, 488–492 (2018)

[33] Nuckols, R.W., Chang, C.-K., Kim, D., Eckert-Erdheim, A., Orzel, D., Baker, L., Baker, T., Wendel, N.C., Quinlivan, B., Murphy, P., *et al.*: Design and evaluation of an independent 4-week, exosuit-assisted, post-stroke community walking program. Annals of the New York Academy of Sciences **1525**(1), 147–159 (2023)

[34] Feng, S., Duarte, M.F.: Few-shot learning-based human activity recognition. Expert Systems with Applications **138**, 112782 (2019)

[35] Ganesha, H., Gupta, R., Gupta, S.H., Rajan, S.: Few-shot transfer learning for wearable imu-based human activity recognition. Neural Computing and Applications **36**(18), 10811–10823 (2024)

[36] Hur, B., Baek, S., Kang, I., Kim, D.: Learning based lower limb joint kinematic estimation using open source imu data. Scientific reports **15**(1), 5287 (2025)

[37] Mihailovic, M., Tonin, L., Tortora, S., Menegatti, E.: Geglu-transformer for imu-to-emg estimation with few-shot adaptation. arXiv preprint arXiv:2604.25670 (2026)

[38] Wesseling, M., Groote, F., Meyer, C., Corten, K., Simon, J.-P., Desloovere, K., Jonkers, I.: Gait alterations to effectively reduce hip contact forces. Journal of Orthopaedic Research **33**(7), 1094–1102 (2015) https://doi.org/10.1002/jor.22852

[39] Astephen, J.L., Deluzio, K.J., Caldwell, G.E., Dunbar, M.J.: Biomechanical changes at the hip, knee, and ankle joints during gait are associated with knee osteoarthritis severity. Journal of Orthopaedic Research **26**(3), 332–341 (2008) https://doi.org/10.1002/jor.20496

[40] Powers, C.M.: The influence of abnormal hip mechanics on knee injury: a biomechanical perspective. J Orthop Sports Phys Ther **40**(2), 42–51 (2010) https://doi.org/10.2519/jospt.2010.3337

[41] Park, J.H., Lee, H., Cho, J.-S., Kim, I., Lee, J., Jang, S.H.: Effects of knee osteoarthritis severity on inter-joint coordination and gait variability as measured by hip-knee cyclograms. Scientific Reports **11**(1) (2021) https://doi.org/10.1038/s41598-020-80237-w

[42] Li, J., Zhu, W., Yang, J., Niu, X., Tang, H., Cao, L., Guo, C.: Degenerative hip osteoarthritis in unilateral knee osteoarthritis patients: A correlation analysis. Orthopaedic Surgery (2025) https://doi.org/10.1111/os.14372

[43] Schmitt, A.C., Baudendistel, S.T., Lipat, A.L., White, T.A., Raffegeau, T.E., Hass, C.J.: Walking indoors, outdoors, and on a treadmill: Gait differences in healthy young and older adults. Gait & Posture **90**, 468–474 (2021) https://doi.org/10.1016/j.gaitpost.2021.09.197